2. STATE OF THE ART

2.1 Physical characteristics of Lidar data within coastal areas

In order to develop a suitable algorithm, which is capable to classify Lidar data (raw 3D Lidar points and their intensity values), the physical characteristics of common Lidar systems as well as the reflection of water and land areas have to be considered. Generally, Lidar systems operate in the near infrared range. Wolfe and Zissis (1989) describe the absorption of infrared radiation depending on the illuminated surface material and the wavelength. They point out that the absorption for water is significantly higher than the absorption for soil. This leads to the fact that the intensity of water points is normally lower than the intensity of land points.
Additionally, as a result of the Rayleigh Criteria, calm water surfaces behave like a mirror. Thus, specular reflection occurs. Often, a distance measurement can not be accomplished successfully because the received radiation energy is not distinguishable from background noise. Hence, the point density of Lidar data within water areas is normally significantly lower than within land areas.

2.2 Systematic changes of intensity and point density depending on the angle of incidence

As pointed out in the previous chapter, intensity and point density depend on the characteristics of the illuminated area. The reflectance of water is lower in case of near infrared light than the reflectance of mudflat. However, also mudflat has quite a smooth surface yielding in similar specular reflection behaviour of the laser beam. Thus, intensity and 2D point density are systematically influenced depending on the angle between the laser beam and the surface normal.

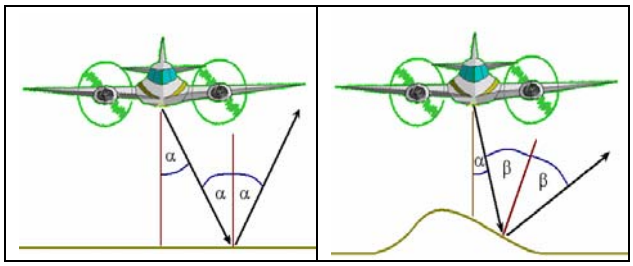

Figure 1. Specular reflection in case of (left) horizontal and (right) tilted area

Figure 1 illustrates how the laser beam is deflected depending on the angle of deflection (α) and the angle of incidence (β), if specular reflection occurs. Assuming that the area of interest is horizontal (which can be stated approximately for large parts of the Wadden Sea) α equals β. In case of tilted regions the surface orientation has to be taken into account in order to calculate β.
Practically, the reflectance behaviour of the laser beam hitting water or mudflat is not exactly equal to specular reflection but similar. Hence, intensity values of points increase, if β decreases. Additionally, more points are measured correctly, if β decreases because the intensity is strong enough to trigger a correct measurement. In order to obtain accurate classification results using intensity and point density, the different reflectance properties of water and mudflat, but also the systematic changes depending on the angle of incidence, have to be taken into account.

2.3 Previous approaches to extract water areas from Lidar data

Brockmann and Mandlburger (2001) developed a technique to extract the boundary between land and river water, and applied it to data from the German river "Oder". Based on Lidar data, the planimetric location of the river centre line as well as bathymetric measurements of the riverbed, the boundary was obtained within a two-stage approach. First, the height level of the water area was derived by averaging the Lidar points in the vicinity of the river centre line. Afterwards, a DTM of all Lidar points (including also points of the water surface) was calculated. Then, the 0 m contour line of the difference model of the Lidar DTM and the water height level was derived. This contour line is called "preliminary borderline". Within step two, the bathymetric points of the preliminary water area were combined with all Lidar points outside the preliminary water area. Then, a DTM representing the riverbeds instead of waterlevel was calculated. Afterwards, the final borderline was obtained by intersecting this DTM including the riverbeds and the height level of water area.
Mandlburger (2006) proposed another method based on the same input data, which also detects the borderline of a river. First, the Lidar points are transformed into the river-axis system. Then, segments with a fixed length in flow direction are created. All points for each segment are used to create a profile across flow direction. After removing all outliers (vegetation and water points etc.), bank slopes of both sides are generated by an adjusted line. Then, one border point for each side is calculated by intersecting these lines with the prior known water height. Finally, all border points are transformed back into project coordinate system and linked.
Brzank and Lohmann (2004) (see also Brzank et al., 2005) developed another algorithm which separates water regions from non-water regions based on a DSM calculated from Lidar data. The main idea is to detect reliable water regions and expand those using height and intensity values. For that purpose, local height minima were extracted from the DSM, which represent potential seed zones of water areas. This step was followed by a region growing procedure using height and intensity data of the DSM grid points. In comparison to the previously mentioned algorithms, no additional information, such as water height or river axis is necessary. However, results were not satisfying, because systematic changes of intensity were not modelled.

2.4 Fuzzy classification concept

In order to classify water points from Lidar data in the Wadden Sea, the first two concepts described in section 2.3 are not sufficient. The algorithm of Brockmann and Mandlburger (2001) as well as Mandlburger (2006) require additional data, such as water height, approximate position of water and bathymetric data. However, these data are not available for the Wadden Sea. Moreover, the algorithms do not use further available information such as intensity and point distribution.
The method of Brzank and Lohmann (2004) is also not sufficient, because systematic changes of intensity are not modelled. Furthermore, the method is not capable of dealing with different water heights within one water region. This remarkable effect occurs, because water height changes over time because of tide. Data of several flight strips are linked together in order to calculate a DSM. The time difference in capturing flight strips can lead to different height levels within one and the same water region.

Figure 2 shows a typical result of function fitting for intensity of both classes. It can be seen that intensity decreases, if the angle of deflection increases.

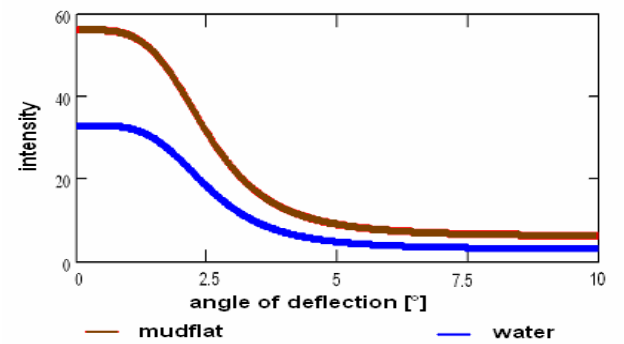

Figure 2. Intensity for both classes as a function of the angle of deflection α

3.1.1 Determination of membership function and their corresponding thresholds

In order to transform a crisp feature value into a fuzzy membership value, a membership function and two thresholds, which limit the application area of the membership function, are needed. We define a straight line as membership function. In case of the feature height the determined mean value of class *mudflat* is used as lower threshold with membership value 0, while the mean value of class *water* is used as upper threshold with membership value 1. In case of intensity and 2D point density, the adjusted functions are used. The individual threshold low (high) of every point equals the adjusted value of function mudflat (water) using the certain angle of the point of interest.

3.1.2 Determination of individual weights

In order to calculate the entire membership value of every point individual weights have to be determined. We define the weight to be in the range of 0 up to 1, where 0 means that the feature is not suited and 1 means that the feature is most useful for classification. For the feature height, only one constant weight is determined, because the height values do not depend on the angle of deflection. In case of intensity and 2D point density an individual weight depending on the angle at the point of interest is obtained. In order to calculate the constant weight of the feature height, all training areas for *water* are combined and the mean $\bar{x}$ and standard deviation $\bar{s}$ is computed. The training areas of *mudflat* are processed in the same way. Then, the values are used to create the Gaussian distribution of the probability density (Figure 3).

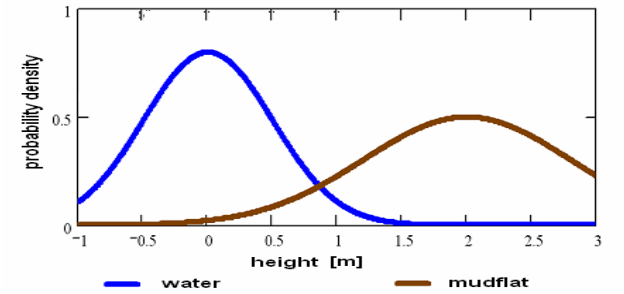

Figure 3. Probability density function of feature height for classes *water* and *mudflat*

It can be stated that the higher the overlapping rate of both distributions the less useful the feature height is to separate between *water* and *mudflat*. Based on this conclusion, the level of significance for the assumption that both distributions are different (H_0: $\bar{x}_{water} \neq \bar{x}_{mudflat}$) is calculated using a statistical test. Equation 3 displays the used test statistics t_f. Then, the corresponding weight is derived from the level of significance by linear interpolation. For that purpose, two constraints are set. If the level of significance is 50% the weight amounts to 0. In case of 100% the weight is 1.

$$t_f = \frac{\bar{x}_{mudflat} - \bar{x}_{water}}{\sqrt{s^2_{\bar{x}_{mudflat}} + s^2_{\bar{x}_{water}}}} = \frac{d}{s_d} \qquad (3)$$

For intensity and 2D point density the determination of the individual weight is very similar. The adjusted values for mudflat and water are calculated using the estimated features of equation 2. The residuals of all observations of one class are used to calculate the standard deviation. Again, both Gaussian distributions are derived and the level of significance is determined leading to the individual weight depending on the angle of deflection of the point of interest.

3.1.3 Determination of water thresholds

After determination of weights the entire membership value of every training point can be calculated using equation 1. Then, the mean of all entire membership values of class *water* and *mudflat* as well as the standard deviation are derived. Now, the two Gaussian distributions of the entire membership value are created. To find the low and high water thresholds the user defines two specific ratios (we normally use 1/10 and 10) of probability density water and probability density mudflat. The values that match these ratios are used as low and high thresholds.

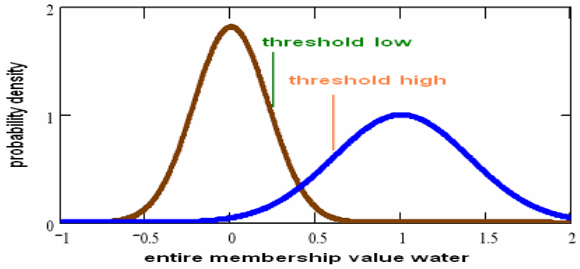

Figure 4. Determination of water threshold low and high

Remark: Generally, a membership value can only lie in the range of 0 to 1. For that reason (see chapter 3.1.1) two thresholds are used in order to limit the use of the membership function. In case of classification all points with feature value below threshold low get a membership value of 0, while all points with feature value above threshold high get a membership value of 1. However, in the analysis of training areas the use of the membership function is not limited leading to membership values below 0 and above 1. This is necessary in order to create normal distributions of the entire membership value *water* (see Figure 4).

4. EXAMPLES

In order to demonstrate the ability of the algorithm, two examples are presented in the section. The first example contains a part of a flight strip of the campaign “Friedrichskoog

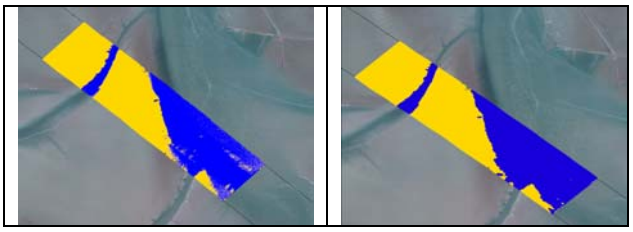

Figure 9. Water (blue) and mudflat (yellow) points after classification (left), additional checks and smoothing (right) - Friedrichskoog

The classification result of campaign "Juist" is visibly slightly better. There are only a few misclassified points due to waves and intensity noise.

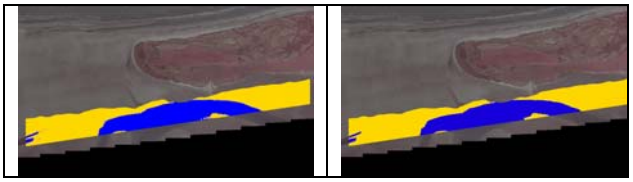

Figure 10. Water and mudflat points after classification (left), additional checks and smoothing (right) – Juist

In order to evaluate the overall correctness, *water* and *mudflat* areas were manually digitized from aerial images and the resulting areas were used as reference for the automatically derived classification. Table 2 lists the results. The correctness of campaign "Juist" is higher than for "Friedrichskoog". Two reasons can be found. On one side, intensity does not differ significantly for all points while point density is not used for the classification "Friedrichskoog". In case of "Juist", all features differ significantly. Furthermore, height increases very slowly at the transition zone from *water* to *mudflat* in case of "Friedrichskoog" making it very difficult to derive correct results. For campaign "Juist" height changes are larger at the transition zone leading to a more accurate classification.

	Friedrichskoog 2005		Juist 2004	
Number of classified points	1.257.518		1.469.405	
Classified water points	592.577		517.858	
Classified land points	664.941		951.547	
	Water	**Land**	**Water**	**Land**
Classified water points	527.641	64.936	510.339	7.519
Classified land points	4.127	660.814	5.886	945.661
Correctness [%]	89.0	99.4	98.5	99.4

Table 2. Evaluated classification results

5. CONCLUSION AND OUTLOOK

A supervised fuzzy classification approach to separate Lidar points into the classes *water* and *mudflat* is introduced. The algorithm is based on the original Lidar data and classifies every flight strip. For the analysis the features height, intensity and 2D point density are used. The classification is based on the fuzzy logic concept. All necessary classification parameters are derived from training areas. Two different examples are presented to illustrate the capability of this algorithm. They demonstrate that the classification algorithm is able to deliver accurate results for different Lidar scanner types.

Future work will focus on the determination of highly precise DTMs for the whole investigated areas. Fur this purpose, bathymetric data has to be included in the calculation in order to fill areas, which are classified as water.

ACKNOWLEDGMENTS

This research has been financed by the Federal Ministry of Education and Research (BMBF) under project no. 03KIS050. We gratefully acknowledge the support of our project partners: Department of Rural Area Husum (ALR), Federal Waterways Directorate (WSD) and the Lower Saxony Water Management, Coastal Defence and Nature Conservation Agency Division Norden-Norderney (NLWKN).

REFERENCES

Brockmann H., Mandlburger G., 2001. Aufbau eines Digitalen Geländemodells vom Wasserlauf der Grenzoder. In *Publikationen der Deutschen Gesellschaft für Photogrammetrie, Fernerkundung und Geoinformationen*, Band 10, 2001, pp. 199 – 208.

Brzank, A., Göpfert, J., Lohmann, P., 2005. Aspects of Lidar Processing in Coastal Areas. In *International Archives of Photogrammetry and Remote Sensing*, Hanover, Germany, Vol. XXXVI PartI/W3, CD , 6 p.

Brzank, A., Lohmann, P., 2004. Steigerung der Genauigkeit von Digitalen Geländemodellen im Küstenbereich aus Laserscannermessungen. In: *Publikationen der Deutschen Gesellschaft für Photogrammetrie, Fernerkundung und Geoinformationen*, Band 13, 2004, pp. 203 – 210.

Brzank, A., Heipke, C., 2006. Classification of Lidar Data into water and land points in coastal areas. In: *The International Archives of Photogrammetry and Remote Sensing,* Bonn, Germany, Vol. XXXVI/3, pp. 197-202.

Katzenbeisser, R. and Kurz, S., 2004. Airborne Laser-Scanning, ein Vergleich mit terrestrischer Vermessung und Photogrammetrie. In: *Photogrammetrie Fernerkundung Geoinformation*, Heft 8, 2004, pp. 179-187.

Kraus K., Pfeifer N., 1998. Determination of terrain models in wooded areas with airborne laser scanner data. In: *ISPRS Journal of Photogrammetry & Remote Sensing*, Volume 53, pp. 193 – 203.

Leckie, D., Cloney, E., Jay, C. and Paradine, D., 2005. Automated Mapping of Stream Features with High-Resolution Multispectral Imagery: An Example of the Capabilities. In: *Photogrammetric Engineering & Remote Sensing*, Vol. 71, No. 2, February 2005, pp. 145 – 155.

Mandlburger, G., 2006. Topographische Modelle für Anwendungen in Hydraulik und Hydrologie. Dissertation, TU Wien. http://www.ipf.tuwien.ac.at/phdtheses/diss_gm_06.pdf (assessed March 29, 2007), 150 p.

Mundt, J. T., Streutker, D. R., Glenn, N. F., 2006. Mapping Sagebrush Distribution Using Fusion of Hyperspectral and Lidar Classifications. In *Photogrammetric Engineering & Remote Sensing*, Vol. 72, No.1, January 2006, pp. 47 – 54.

Wolfe, W. and Zissis, G.J. 1989. The infrared handbook. The Infrared Information Analysis Center. Enviromental Research Institut of Michigan, Detroit, 1700 p.